This article was downloaded by: [Renmin University of China]
On: 13 October 2013, At: 10:51
Publisher: Taylor & Francis
Informa Ltd Registered in England and Wales Registered Number: 1072954 Registered office: Mortimer House, 37-41 Mortimer Street, London W1T 3JH, UK

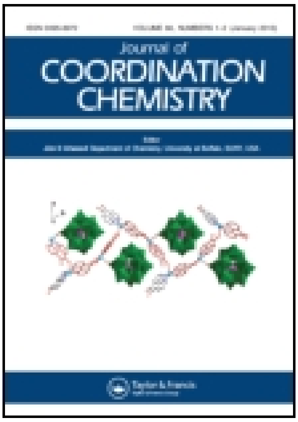

Journal of Coordination Chemistry
Publication details, including instructions for authors and subscription information:
http://www.tandfonline.com/loi/gcoo20

Copper(II) and molybdenum(VI) complexes with 5-bromosalicylaldehyde S-allylisothiosemicarbazone: Syntheses, characterizations and crystal structures

REZA TAKJOO [a] , ALIREZA HASHEMZADEH [a] , HADI AMIRI RUDBARI [b] & FRANCESCO NICOLÒ [b]

[a] Department of Chemistry , School of Sciences, Ferdowsi University of Mashhad , Mashhad , Iran

[b] Dipartimento di Chimica Inorganica , Chimica Analitica e Chimica Fisica Università di Messina , Contrada Papardo , Messina , Italy

Accepted author version posted online: 08 Nov 2012.Published online: 23 Jan 2013.

To cite this article: REZA TAKJOO , ALIREZA HASHEMZADEH , HADI AMIRI RUDBARI & FRANCESCO NICOLÒ (2013) Copper(II) and molybdenum(VI) complexes with 5-bromosalicylaldehyde S-allylisothiosemicarbazone: Syntheses, characterizations and crystal structures, Journal of Coordination Chemistry, 66:2, 345-357, DOI: 10.1080/00958972.2012.748191

To link to this article: http://dx.doi.org/10.1080/00958972.2012.748191

PLEASE SCROLL DOWN FOR ARTICLE

Taylor & Francis makes every effort to ensure the accuracy of all the information (the “Content”) contained in the publications on our platform. However, Taylor & Francis, our agents, and our licensors make no representations or warranties whatsoever as to the accuracy, completeness, or suitability for any purpose of the Content. Any opinions and views expressed in this publication are the opinions and views of the authors, and are not the views of or endorsed by Taylor & Francis. The accuracy of the Content should not be relied upon and should be independently verified with primary sources of information. Taylor and Francis shall not be liable for any losses, actions, claims, proceedings, demands, costs, expenses, damages, and other liabilities whatsoever or howsoever caused arising directly or indirectly in connection with, in relation to or arising out of the use of the Content.

Journal of Coordination Chemistry
Vol. 66, No. 2, 20 January 2013, 345–357

Taylor & Francis
Taylor & Francis Group

Copper(II) and molybdenum(VI) complexes with 5-bromosalicylaldehyde *S*-allylisothiosemicarbazone: Syntheses, characterizations and crystal structures

REZA TAKJOO[†]*, ALIREZA HASHEMZADEH[†], HADI AMIRI RUDBARI[‡] and FRANCESCO NICOLÒ[†]

[†]*Department of Chemistry, School of Sciences, Ferdowsi University of Mashhad, Mashhad, Iran;* [‡]*Dipartimento di Chimica Inorganica, Chimica Analitica e Chimica Fisica Università di Messina, Contrada Papardo, Messina, Italy*

(*Received 17 June 2012; in final form 20 September 2012*)

A new tridentate Schiff base, 5-bromosalicylaldehyde *S*-allylisothiosemicarbazone hydrobromide (H_2L), and several new mononuclear complexes of copper(II) and molybdenum(VI) of this ligand with general formulas ([Cu(L)Im] (**1**)), ([Cu(L)NH_3]·4H_2O (**2**)), and ([MoO_2(L)1-MeIm] (**3**), Imidazole: Im, 1-methylimidazole: 1-MeIm) were prepared and characterized by elemental analyses, IR, Proton Magnetic Resonance Spectroscopy and Ultraviolet-visible techniques. The physico-chemical results suggested that the H_2L coordinates in the dianionic tridentate form. Crystal structures of the Cu(II) complexes reveal a square planar configuration surrounded by the dianionic tridentate isothiosemicarbazone (ONN) and Im and NH_3 for **1** and **2**, respectively. The L^{2-}, two oxo, and 1-methylimidazole are coordinated to molybdenum(VI) in a distorted octahedral geometry in **3**. Formation of pure metal oxide residues was confirmed by thermal degradation of the complexes.

Keywords: Schiff base; Isothiosemicarbazone; Copper and molybdenum complexes; TGA; Crystal structure

1. Introduction

Complexes of palladium and nickel with thiosemicarbazide were synthesized by Jensen *et al*. [1, 2]. Reaction of thiosemicarbazide with alkyl halides produces isothiosemicarbazides which can participate in condensation reactions with aldehydes and ketones, producing isothiosemicarbazones [3–5]. Alkylation of sulfur makes the isothioamidic nitrogen a better donor [6]. Tridentate isothiosemicarbazides are usually coordinated to the metal *via* isothioamide nitrogen, azomethine nitrogen, and related heteroatoms of aldehydes or ketones (XNN donor set, X = N or O). Numerous structures of tridentate isothiosemicarbazone complexes were determined [1]. In general, isothiosemicarbazides or their derivatives in the complexes show antimicrobial, antituberculosis [7, 8], antileukemia [9, 10], antibacterial, and antifungal activities [11]. The kind of aldehydes or ketones used to prepare isothiosemicarbazones or different metal centers such as molybdenum or copper will affect their

---

*Corresponding author. Email: r.takjoo@um.ac.ir

Journal of Coordination Chemistry
ISSN 0095-8972 print/ISSN 1029-0389 online © 2013 Taylor & Francis
http://dx.doi.org/10.1080/00958972.2012.748191

biological activities [12], although sometimes similarities could be found [13, 14]. N-donor ligands such as imidazole and its derivatives can improve the bioactivities of mixed ligand complexes [15]. Compounds containing amine groups such as NH_3 and imidazole derivatives can make supramolecular structures and are used in crystal engineering architectures [16]. In addition, imidazole derivatives in complexes have enzyme properties [17].

Some copper sites have antibacterial, antifungal, and anticancer properties [18]. Mixed ligand copper(II) complexes with N-donors such as imidazole have been considered as 'model compounds' [19, 20]. Also, the active site of some metalloenzymes contain copper (II) [21].

Mo complexes which can change their metal oxidation number can have some oxidoreductases, hydrogenase, xanthine oxidase, DMSO reductase, and other oxo-transferase properties [22]. Moreover, molybdenum complexes [*cis*-MoO_2(L)D], D can be a solvent, are useful due to easy replacement of the solvent. Molybdenum(VI) complexes participate in sulfite oxidase, DMSO reductase, aldehyde oxidoreductase, and nitrate reductase reactions [23–25].

Here, we report 5-bromosalicylaldehyde *S*-allylisothiosemicarbazone hydrobromide (H_2L) (Scheme 1) and its [Cu(NH_3)L]·$4H_2O$ (**1**), [Cu(Im)L] (**2**) and [MoO_2(1-MeIm)L] (**3**) (Im: imidazole, 1-MeIm: 1-methylimidazole) complexes. All compounds were thoroughly characterized by elemental analyses, IR, Proton Magnetic Resonance Spectroscopy (^{1}H NMR), and Ultraviolet-visible (UV-Vis) methods; in the case of the complexes, X-ray crystallography and thermogravimetric analysis were done as well.

2. Experimental

2.1. *Reagents and physical measurements*

All compounds were purchased from commercial sources and used without purification. Elemental analyses (C, H, N, and S) were performed on a Thermo Finnigan Flash Elemental Analyzer 1112EA. IR spectra from 400 to 4000 cm^{-1} were recorded in KBr pellets on a Buck 500 Scientific spectrometer. ^{1}H NMR spectra of DMSO-d_6 solutions were recorded on a Bruker BRX 100 AVANCE with the signal of the free DMSO at 2.49 ppm as a reference. Electronic spectra were measured with a SHIMADZU model 2550 UV–Vis spectrophotometer (250-1100 nm) in DMF. The TGA diagrams were recorded in a TGA-50 SHIMADZU instrument at a heating rate of 10 °C/min under air from 20 to 950 °C.

2.2. *5-Bromo S-allylisothiosemicarbazone hydrobromide (H_2L)*

Allyl bromide (1.1 g, 9.0 mmol) was added to an ethanolic solution (5 mL) of thiosemicarbazide (0.82 g, 9.0 mmol) and refluxed for 10 min on a water bath at *ca*. 90 °C. 5-Bromosalicylaldehyde (1.8 g, 9.0 mmol) was then mixed to the resulting solution and the reflux

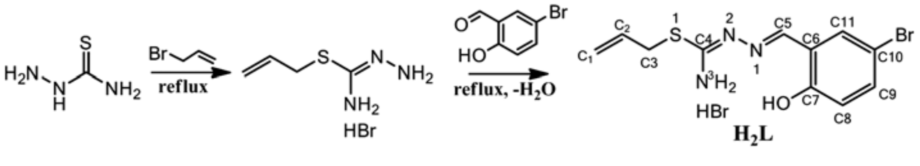

Scheme 1. Synthesis of 5-bromosalicylaldehyde *S*-allylisothiosemicarbazone hydrobromide (H_2L).

was continued for an additional 30 min. A yellow precipitate was separated by filtration, washed with ethanol, and dried in air. Yellow. Yield: 2.8 g, 78.7%. m.p.: 216 °C. Anal. Calcd for $C_{11}H_{13}Br_2N_3OS$ (392.76 g mol^{-1}): C, 33.44; H, 3.32; N, 10.63; S, 8.12. Found: C, 32.80; H, 3.31; N, 10.41; S, 8.02%. IR (KBr) cm^{-1}: *ν*(OH) 3336, *ν*(NH) 3268 m, 3173s, *ν*(C=N) 1542 m, 1623s, *ν*(C=C) 1474 m, *ν*(C–O) 1235 m, *ν*(N–N) 1097 m. UV/Vis (DMF) λ_{max}, nm (logε, L mol^{-1} cm^{-1}): 266 (4.38), 304 (4.62), 314 (4.62), 346 (4.74). ^{1}H NMR (100 MHz, DMSO-d$_6$): $\delta = 11.4$, 10.8 (s, 1H, OH), 9.8 (s, 2H, N^{3}H), 8.7 (s, 1H, C^{5}H), 8.2 (d, 1H, C^{11}H), 7.5 (dd, 1H, C^{9}H), 6.9 (d, 1H, C^{8}H), 5.7-6.1 (m, 1H, C^{2}H), 5.3 (t, 2H, C^{1}H), 4.1 (d, 2H, C^{3}H).

2.3. *Synthesis of complexes*

2.3.1. [Allyl[(5-bromo-2-hydroxyphenyl)methylene]hydrazincarboximidothioato(-2)-N, N^2,O^2]ammonia-copper, tetrahydrate (1). A mixture of H_2L (0.034 g, 0.1 mmol) and a molar excess of ammonia 25% (0.1 mL, 5.7 mmol) were dissolved in ethanol (5 mL). $CuCl_2 \cdot 2H_2O$ (0.017 g, 0.1 mmol) was added to the solution. The reaction mixture was stirred and refluxed for 1 h. After standing at room temperature for one week, crystals were formed from the resulting clear green solution. The crystalline product was collected, washed with cold ethanol, and dried in air. $[Cu(NH_3)L]\cdot 4H_2O$ (1): irregular, green. Yield: 0.023 g, 59.0%. m.p.: 163 °C. Anal. Calcd for $C_{11}H_{13}BrCuN_4OS \cdot 4H_2O$ (464.82 g mol^{-1}): C, 27.42; H, 4.55; N, 12.05; S, 6.90. Found: C, 27.51; H, 4.59; N, 12.13; S, 6.93%. IR (KBr) cm^{-1}: *ν*(OH) 3419 m, *ν*(NH) 3149s, *ν*(C=N) 1605 m, *ν*(C=C) 1507 m, *ν*(C–O) 1090 m, *ν*(N-N) 1024 m. UV/Vis (DMF) λ_{max}, nm (logε, L mol^{-1} cm^{-1}): 326 (4.11)sh, 336 (4.12), 348 (3.27).

2.3.2. [Allyl[(5-bromo-2-hydroxyphenyl)methylene]hydrazincarboximidothioato(-2)-N, N^2,O^2]imidazole-copper (2). $Cu(CH_3COO)_2 \cdot H_2O$ (0.20 g, 1 mmol) was added to a mixture of H_2L (0.034 g, 0.1 mmol) and imidazole (0.20 g, 3 mmol) in EtOH (5 mL). The mixture was heated under reflux for 45 min, then cooled, and allowed to stand in air for several days. Red crystals were collected, washed (EtOH), and dried in air. [Cu(Im)L] (2): irregular, green. Yield: 0.026 g, 59.1%. m.p.: 184 °C. Anal. Calcd for $C_{14}H_{14}BrCuN_5OS$ (443.81 g mol^{-1}): C, 37.89; H, 3.18; N, 15.78; S, 7.22. Found: C, 38.03; H, 3.11; N, 15.99; S, 7.27%. IR (KBr) cm^{-1}: *ν*(NH) 3411s, *ν*(C=N) 1579 m, *ν*(C=C) 1491 m, 1437w, *ν*(C=N) 1535s, *ν*(Im) 1249w, *ν*(C–O) 1172 m, *ν*(N–N) 1056 m. UV/Vis (DMF) λ_{max}, nm (log ε L mol^{-1} cm^{-1}): 336 (4.00)sh, 350 (4.08), 400 (4.32), 584 (2.02)sh.

2.3.3. [Allyl[(5-bromo-2-hydroxyphenyl)methylene]hydrazincarboximidothioato(-2)-N, N^2,O^2]dioxido(1-methylimidazole)-molybdenum (3). To a boiling ethanol solution (6 mL) of the H_2L (0.034 g, 0.1 mmol) and 1-methylimidazole (0.25 g, 3 mmol), a 5 mL ethanolic solution of MoO2 (acac)2 (0.33 g, 1mmol) was added to a boiling ethanolic solution (6 mL) of the H2L (0.034 g, 0.1 mmol) and 1-methylimidazole (0.25 g, 3mmol). This solution was refluxed for 1 h. The deep red solution was allowed to stand in air for one week. The crystalline red complex was separated, washed with ethanol, and dried in air. $[MoO_2(1\text{-}MeIm)L]$ (3): Irregular, red. Yield: 0.037 g, 72.6%. m.p.: 207 °C. Anal. Calcd for $C_{15}H_{16}BrMoN_5O_3S$ (522.25 g mol^{-1}): C, 34.50; H, 3.09; N, 13.41; S, 6.14. Found: C, 34.68;

H, 3.11; N, 13.47; S, 6.18%. IR (KBr) cm^{-1}: ν(NH) 3421s, ν(C=N) 1564 m, 1632 m, ν(C=C) 1488 m, ν(C=N) 1535s, ν(1-MeIm) 1257w, ν(C–O) 1185w, ν(N–N) 1036 m. UV/Vis (DMF) λ_{max}, nm (log ε L mol^{-1} cm^{-1}): 304 (4.34), 340 (4.08)sh, 438 (3.59). ^{1}H NMR (100 MHz, DMSO-d$_6$): $\delta = 9.4$ (s, 1H, N^{3}H), 8.5 (s, 1H, C^{5}H), 7.8 (s, 1H, C^{14}H), 7.6 (d, 1H, C^{11}H), 7.5 (d, 1H, C^{12}H), 7.1 (s, 1H, C^{9}H), 6.9 (d,1H, C^{8}H), 6.75 (d,1H, C^{13}H), 5.8-6.1 (m, 1H, C^{2}H), 5.2 (t, 2H, C^{1}H), 3.8 (d, 2H, C^{3}H), 3.65 (s, 3H, C^{15}H$_3$).

2.4. *Structure determination*

Data were collected at room temperature with a Bruker APEX II CCD area-detector diffractometer using MoK$_\alpha$ radiation ($\lambda = 0.71073$ Å). Data collection, cell refinement, data reduction, and absorption correction were performed using multiscan methods with Bruker software [26]. The structures were solved by direct methods using SIR2004 [27]. The non-hydrogen atoms were refined anisotropically by the full matrix least squares method on F^2 using SHELXL [28]. All hydrogens were placed at calculated positions and constrained to ride on their parent. The details concerning collection and analysis are presented in table 1.

3. Results and discussion

The physical and analytical data for all compounds are listed in the Experimental section. Table 2 shows a comparison of spectral characterizations between the compounds.

H$_2$L, 5-bromosalicylaldehyde *S*-allylisothiosemicarbazone hydrobromide, was synthesized by *S*-alkylation of thiosemicarbazide with allyl bromide and then condensation of the resulting *S*-allylisothiosemicarbazone hydrobromide with 5-bromosalicylaldehyde to produce the product in good yield (scheme 1).

The complexes were formed by direct reaction of H$_2$L, a dianionic tridentate NNO donor, with imidazole solution (ammonia or 1-methylimidazole) and finally the corresponding metal salts. The materials are stable in air. The physical and analytical results are compatible with the empirical formulas.

3.1. *Spectral studies*

In order to elucidate H$_2$L coordination to metal ions, the important bands in the IR spectra of the ligand and its complexes are compared with each other.

In the ligand, the band at 3336 cm^{-1} can be assigned to ν(OH) [29, 30]. After complexation, this band disappears, confirming that coordination takes place *via* phenolic oxygen [31]. In the ligand spectrum, strong and weak peaks at 3268 and 3173 cm^{-1} [32] are assigned to asymmetric and symmetric vibrations of N^{4}H$_2$, respectively. These peaks shift to lower frequencies after coordination [33, 17]. A new band in the IR spectrum of the complexes is seen at 3411 cm^{-1} for ν(NH).

The azomethine and isothioamide combined absorption of the free ligand, ascribed to δ(NH$_2$) and ν(N^2=C^4), appear at 1623 and 1542 cm^{-1}, respectively [34].

A shoulder at 1593 cm^{-1} can be attributed to the aryl-C^5=N^1-N^2- stretching vibration in H$_2$L [35].

The aromatic and allylic C=C absorptions generally appear at 1450–1600 cm^{-1} [17]. After coordination, the phenolic O–H deformation band at 1408 cm^{-1} is not present and the

Table 1. Crystal, collection, and refinement data for **1-3**.

	1	**2**	**3**
Empirical formula	$C_{22}H_{26}Br_2Cu_2N_8O_2S_2{\cdot}4H_2O$	$C_{28}H_{28}Br_2Cu_2N_{10}O_2S_2$	$C_{15}H_{16}BrMoN_5O_3S$
Formula weight	856.58	887.62	522.24
Temperature (K)	293(2)	296(2)	296(2)
Wavelength (Å)	0.71073	0.71073	0.71073
Crystal system	Monoclinic	Monoclinic	Monoclinic
Space group	P2(1)/*n*	P2(1)/*n*	P2(1)/*n*
Unit cell dimensions	$a = 10.5875(6)$ Å $b = 19.8013(11)$ Å $c = 16.7014(10)$ Å $\beta = 106.593(2)°$	$a = 12.1513(3)$ Å $b = 8.2481(2)$ Å $c = 17.3218(4)$ Å $\beta = 103.6770(10)°$	$a = 8.7847(2)$ Å $b = 22.4449(5)$ Å $c = 9.8363(2)$ Å $\beta = 102.8790(10)°$
Volume (Å^3)	3355.6(3)	1686.85(7)	1890.65(7)
Z, Calculated density (Mg/m^3)	4, 1.696	2, 1.748	4, 1.835
Abs. coeff. (mm^{-1})	3.820	3.797	2.943
F(000)	1716	884	1032
Crystal size (mm)	0.26 × 0.14 × 0.10	0.22 × 0.12 × 0.07	0.23 × 0.08 × 0.05
Theta range for data collection	1.64 to 25.00°	2.33 to 27.53°	2.81 to 27.00°
Limiting indices	−9<=h<=12, −23<=k<=23,−19<=l<=19	−15<=h<=15, −10<=k<=10,−22<=l<=22	−11<=h<=11, −28<=k<=28,−10<=l<=12
Reflections collected/unique	25,505 / 5896 [R(int) = 0.0446]	21,508 / 3881 [R(int) = 0.0337]	44,309 / 4125 [R(int) = 0.0452]
Comp. to theta = 27.53	99.8%	99.8%	99.9%
Refinement method	Full-matrix least-squares on F^2	Full-matrix least-squares on F^2	Full-matrix least-squares on F^2
Data/restraints/ parameters	5896/2/413	3881/1/212	4125/1/240
Goodness-of-fit on F^2	1.019	1.062	1.042
Final *R* indices [I > 2sigma(I)]	R1 = 0.0453, *w*R2 = 0.1142	R1 = 0.0304, *w*R2 = 0.0762	R1 = 0.0292, *w*R2 = 0.0641
R indices (all data)	R1 = 0.0785, *w*R2 = 0.1333	R1 = 0.0436, *w*R2 = 0.0849	R1 = 0.0461, *w*R2 = 0.0704

phenolic C-O band at 1235 cm^{-1} in the free ligand shifts to lower frequency in the metal-ion complexes [35]. These are strong evidence for ligand coordination to the metal ions *via* phenolic oxygen. The ν(N–N) vibration at 1097 cm^{-1} in the ligand spectrum is shifted to higher and lower frequency in Cu- and Mo-complexes, respectively.

^{1}H NMR spectra of the ligand and Mo-complex in DMSO-d$_6$ show narrow signals. The ligand can show *syn*/*anti* and *cis*/*trans* isomers, resulting from different arrangements of various groups around the C=N double bond [36]. ^{1}H NMR spectra can be used to investigate and identify the intermolecular interactions in isothiosemicarbazones including O–H···N^1 and N^1···N^4–H, *syn*/*anti* isomer around C=N^1 bond and *cis*/*trans* isomer around N^2=C [37,38].

The ligand spectrum shows singlets at δ 11.4 and 10.8 ppm, attributed to OH. The existence of these two different signals confirms the presence of *syn*/*anti* isomers in solution [37,39]. The ratio of 26 : 74 in the ^{1}H NMR data demonstrates the ratio of *syn*/*anti* isomers. The more downfield OH signals may be due to hydrogen bonding interactions and loss of electron density. The OH bands disappear in the Mo-complex spectrum indicating that ligand deprotonation resulted from metal chelation.

H_2L shows a sharp singlet with an integration of two at δ 9.8 ppm, which is ascribed to the isothioamidic NH_2 protons [37]. This singlet shows *cis* and *trans* tautomers in solution [40]. This proton is shifted to upfield after H_2L coordination by 0.4 ppm revealing that the

Table 2. Color, melting point, selected IR bands and electronic spectra.

			IR bands (cm^{-1})					
Compounds	Colors	m.p. (°C)	νOH	νN^4H_2	$\delta NH_2 + \nu N^2 = C^4$	νCO	νNN	Electronic spectra (λ_{max} [nm])
H_2L	Yellow	216	3336	3268, 3173	1623, 1542	1235	1097	266 (4.38), 304 (4.62), 314 (4.62), 346 (4.74)
1	Green	163	3419	3149	1605	1090	1025	326 (4.11)sh, 336 (4.12), 348 (3.27)
2	Green	184	–	3411	1579	1172	1056	336 (4.00)sh, 350 (4.08), 400 (4.32), 584 (2.02)sh
3	Red	207	–	3421	1632, 1564	1185	1036	304 (4.34), 340 (4.08)sh, 438 (3.59)

Table 3. Selected bond lengths (Å) and angles (°) for **1-3** with esd's in parentheses.

Distances (Å)		Angles (°)	
1			
Cu1-N1	1.948(5)	N1-Cu1-N3	80.0(2)
Cu1-N3	1.935(4)	N3-Cu1-N4	95.3(2)
Cu1-N4	1.998(5)	N4-Cu1-O1	91.4(2)
Cu1-O1	1.922(3)	O1-Cu1-N1	93.3(2)
C7-N1	1.280(8)	C5-N1-N2	117.8(5)
N1-N2	1.382(5)	N1-N2-C4	108.9(5)
N2-C4	1.322(8)	N2-C4-S1	110.8(4)
C4-N3	1.292(7)	N2-C4-N3	123.5(5)
C4-S2	1.776(5)	S1-C4-N3	125.5(4)
2			
Cu1-N1	1.954(2)	N1-Cu1-N3	80.50(8)
Cu1-N3	1.951(2)	N3-Cu1-N4	97.63(9)
Cu1-N4	1.975(2)	N4-Cu1-O1	90.48(8)
Cu1-O1	1.913(2)	O1-Cu1-N1	91.40(8)
C5-N1	1.280(3)	C5-N1-N2	117.1(2)
N1-N2	1.392(3)	N1-N2-C4	109.6(2)
N2-C4	1.315(3)	N2-C4-S1	111.0(2)
C4-N3	1.322(3)	N2-C4-N3	123.5(2)
C4-S1	1.770(2)	S1-C4-N3	125.5(2)
3			
Mo1-N4	2.391(3)	O3-Mo1-N4	167.1(1)
Mo1-O2	1.712(2)	N1-Mo1-N4	77.92(9)
Mo1-O3	1.697(2)	N3-Mo1-N4	81.1(1)
Mo1-O1	1.943(2)	O2-Mo1-N4	86.5(1)
Mo1-N1	2.254(2)	O1-Mo1-N4	77.20(9)
Mo1-N3	2.030(3)	O1-Mo1-N3	148.3(1)
C5-N1	1.280(4)	N1-Mo1-O2	160.3(1)
N1-N2	1.399(4)	O3-Mo1-O1	96.6(1)
N2-C4	1.301(4)	O3-Mo1-N1	90.2(1)
C4-N3	1.345(4)	O3-Mo1-N3	99.7(1)
C4-S1	1.753(3)	O3-Mo1-O2	106.2(1)

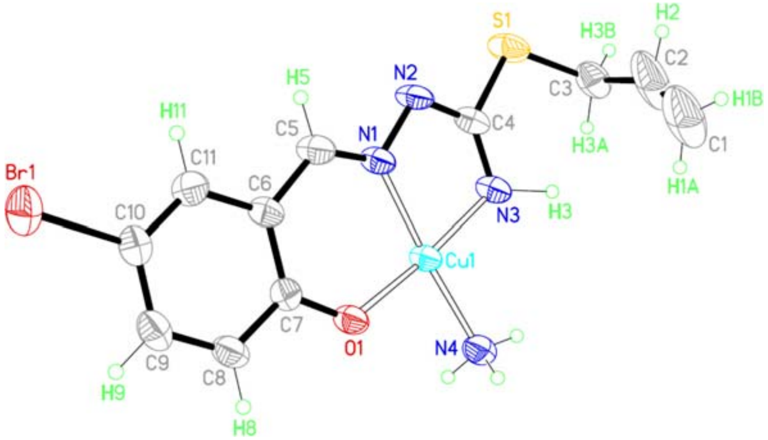

Figure 1. ORTEP drawing with atom numbering of one of the two crystallographically independent units of **1**. Displacement ellipsoids are drawn at 30% probability level and hydrogens are shown as small spheres of arbitrary radii. The water molecules are not shown for clarity.

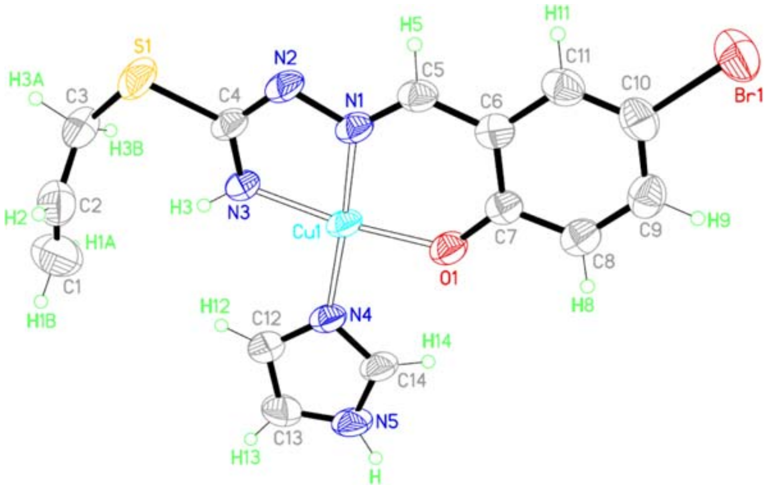

Figure 2. ORTEP drawing of **2** with atom numbering. Displacement ellipsoids are drawn at 50% probability level and hydrogens are shown as small spheres of arbitrary radii.

ligand binds to the metal ion *via* the isothioamidic nitrogen. Signals at δ 8.7 and 8.5 ppm are attributed to the azomethine in the ligand and Mo(VI)-complex spectra, respectively. The upfield shift from δ 8.7 ppm to 8.5 ppm confirms coordination through the azomethine nitrogen [41]. The protons of the phenyl ring are not chemically and magnetically equivalent, and have three different signals at δ 6.9, 7.5, and 8.2 ppm, corresponding to C^8H, C^9H, and $C^{11}H$, respectively [42]. The C^1H proton is found at δ 5.3 and 5.2 ppm as a triplet in the ligand and complex, respectively. In H_2L and the molybdenum complex, the signals at δ 5.7–6.1 and 3.8–4.1 ppm are assigned to C^2H and C^3H protons, respectively [34].

The electronic spectrum of H_2L in DMF indicates four bands at 260–380 nm. The first two bands at 266 and 304 nm are attributed to $\pi \rightarrow \pi^*$ transitions of the aromatic rings, and azomethinic and isothioamidic moieties, respectively [43]. The two other bands at 314 and 346 nm have been assigned to $n \rightarrow \pi^*$ transitions of azomethinic and isothioamidic moieties, respectively [44, 45]. After H_2L coordination, a blue shift occurred for the $\pi \rightarrow \pi^*$ transitions; however, it could not be detected in DMF solution due to a shift to lower wavelengths. On the other hand, the $n \rightarrow \pi^*$ transitions are shifted to lower energy. The reason for these changes is related to electron density variation after coordination. In other words, despite n orbitals, the π orbitals are more stable after complexation.

Spectra of the complexes show LMCT charge transfer bands at 348–438 nm. Three transitions as ${}^2B_{1g} \rightarrow {}^2B_{2g}$, ${}^2B_{1g} \rightarrow {}^2A_{1g}$, and ${}^2B_{1g} \rightarrow {}^2E_g$ are expected for a square planar geometry of copper complexes [30]. However, due to extension of charge transfer transition to low-energy visible region, only one transition can be seen at 584 nm for 2. The lack of electrons in the 4d electronic configuration of Mo(VI) leads to absence of d–d transitions in the visible region.

3.2. *Thermal studies*

The TGA curve of the powder of 1 in air shows four steps on the DrTGA curve at 20–270 °C, 280–550 °C, 550–690 °C, and 660–700 °C. In the first stage, waters are eliminated with a weight loss of 15.4% (Calcd 15.5%). The second stage of thermal decomposition is attributed to removal of ammonia with a weight loss of 3.7% (Calcd 3.66%). The complex loses 45.74% (Calcd 45.62%) of weight with the removal of the remaining organic part in the third step. Finally, the CuO remains after 79.89% (Calcd 80.14%) weight loss of the initial material.

For 2, three stages are detected at 160–230 °C, 260–385 °C, and 495–685 °C. The first peak in the thermogram, having a maximum at 200 °C, shows a weight loss of 18.10% (Calcd 18.0%) due to loss of Br. In the second step, allyl is removed with weight loss of 9.30% (Calcd 9.25%). The major mass decrease occurs at 520–569 °C which is related to decomposition of 2 to CuO with a weight loss of 18.11% (Calcd 17.91%).

The TG/DTG curve of **3** exhibits four decomposition steps at 160–230 °C, 310–390 °C, 435–565 °C, and 670–760 °C. At 160–230 °C (maximum 212 °C), the elimination of Br occurs with a 14.82% (Calcd 15.32%) weight loss. The allyl fragment is removed in the second step (8.0% weight loss (Calcd 7.86%)). In the third step, the residue shows about 56.11% (Calcd 58.46%) weight loss due to decomposition of the remaining organic part; and finally, the conversion to MoO_2 at 520–695 °C is confirmed by the last TGA peak.

The decomposition products of **2** and **3** are similar – Br, allyl moiety, and finally metal oxide. However, for **1**, water, ammonia, and CuO are products of the thermal degradation process.

3.3. *Structure of the complexes*

Data summary of crystallographic parameters are given in table 1. Relevant bond lengths and angles are given in table 3. The thermal ellipsoid ORTEP images of the complexes with their atom numbers are shown in figures 1–3.

The ligand is a tridentate dianionic ONN donor, using a phenolic oxygen, azomethine nitrogen, and deprotonated isothioamide nitrogen, coordinated to metal by forming stable five- and six-membered rings. As ONN donors are situated on the same side, the ligand

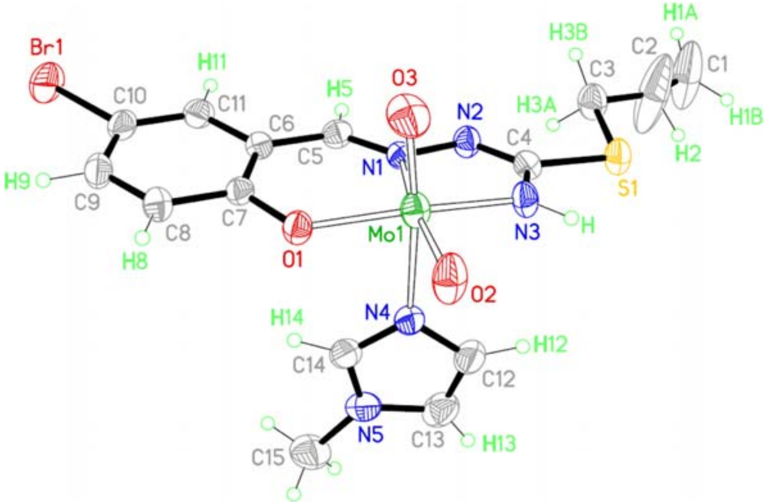

Figure 3. ORTEP drawing of **3** with atom numbering. Displacement ellipsoids are drawn at 50% probability level and hydrogens are shown as small spheres of arbitrary radii.

shows *syn* and *trans* configuration about C4–N2 and C5–N1, respectively. Decrease in the thioamide C4=N3 bond length in the complexes compared to free isothiosemicarbazone shows that deprotonation occurs through H_2L coordination *via* the isothioamide nitrogen. In the complexes, azomethine C5=N1 bonds are equal and C4=N3 and N1–N2 bond lengths increase. The C–S and N–N bond distances are similar to and smaller than those of their analogous isothiosemicarbazone complexes, respectively [3].

Complexes **1** and **2** adopt distorted square-planar geometries surrounded by an N-donor ligand and the dianionic tridentate L^{2-} which coordinates through its [ONN] donor set; for the molybdenum bis-oxo complex (**3**), L^{2-}, two oxo, and 1-methylimidazole are coordinated in a distorted octahedron. Deviation of the copper(II) complexes from square planar (the N1N3N4O1 plane) is negligible. In 1, the asymmetric unit contains two neutral complexes and four waters. There are four hydrogen bonds, N2···Hw3–Ow2 (2.769(6) Å), N2A···Hw2–Ow3 (2.833(7) Å), O1···Hw4–Ow2 (2.720(6) Å), and O1A···Hw1–Ow3 (2.839(6) Å), for

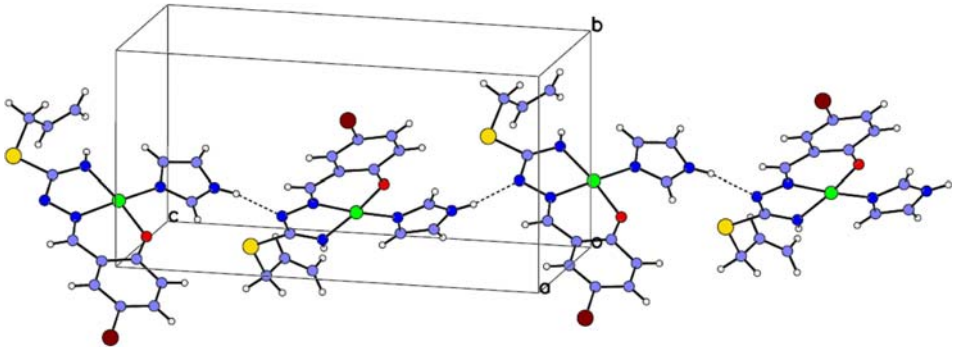

Figure 4. The N5–H…N2 (2.799(3) Å) hydrogen bonding expands the network along the bisector angle of *bc* plane as 1-D in **2**.

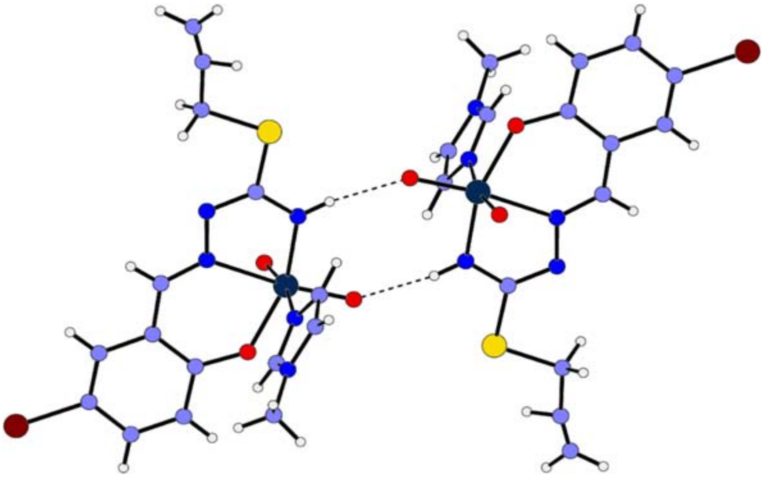

Figure 5. A view of the dimer of **3** with $R^2_2(8)$ graph-set motifs. Note: Hydrogen bonds are shown as dashed lines.

Table 4. Details of hydrogen bonding.

Compounds		*d*(D–H)	*d*(D...A)	D–H...A	∠(DHA)
1	OW2–HW3...N1	0.870(.064)	3.764(.006)	2.948(.062)	157.01(5.83)
	OW2–HW3...N2	0.870(.064)	2.769(.006)	1.906(.065)	171.25(6.52)
	OW3–HW2...N2A	0.882(.033)	2.834(.007)	1.957(.031)	172.69(2.58)
	OW3–HW2...N1A	0.882(.033)	3.796(.006)	2.988(.028)	153.21(2.22)
	C9–H9B...OW1	0.970(.009)	3.665(.020)	2.779(.017)	152.16(0.64)
	N3–H3...OW1	0.860(.005)	3.125(.019)	2.328(.019)	154.32(0.46)
	N4–H4A...OW1	0.890(.005)	3.325(.019)	2.493(.019)	155.87(0.51)
	N4A–H4A2...S2	0.890(.005)	3.611(.005)	2.759(.002)	160.72(0.29)
	C7–H6...OW	0.930(.005)	3.729(.008)	2.803(.006)	174.44(0.35)
	OW2–HW4...O1	1.024(.076)	2.720(.006)	1.752(.075)	156.21(6.49)
	OW3–HW1...O1A	0.889(.087)	2.839(.006)	1.977(.092)	163.05(8.60)
	C7A–H20...OW	0.930(.006)	3.710(.009)	2.875(.007)	150.17(0.37)
	N4A–H4A1...Br1A	0.890(.005)	3.838(.005)	2.998(.001)	158.08(0.31)
2	N5–H...N1	0.860(.002)	3.778(.003)	2.940(.002)	165.19(0.14)
	N5–H...N2	0.860(.002)	2.799(.003)	1.950(.002)	168.88(0.15)
	C3–H3B...O1	0.970(.003)	3.485(.004)	2.531(.002)	167.70(0.18)
3	C11–H11...O3	0.930(.003)	3.708(.004)	2.803(.003)	164.74(0.19)
	C9–H9...O3	0.930(.003)	3.713(.004)	2.857(.003)	153.49(0.20)
	C15–H15B...N2	0.960(.004)	3.759(.005)	2.856(.002)	157.23(0.24)
	N3–H...O2	0.866(.027)	2.951(.003)	2.093(.028)	170.41(2.66)

two molecules in the asymmetric unit, playing an important role in lattice expansion. In **2**, the asymmetric unit contains a neutral molecule. The N5–H…N2 (2.799(3) Å) hydrogen bond expands the network along the bisector angle of the *bc* plane in 1-D (figure 4).

A Schiff base (NNO donor), two oxo, and a 1-methylimidazole occupy six sites of metal coordination in **3**. The angles and distances of *cis*-MoO_2 unit are 106.2(1)°, 1.697 (2) Å, and 1.712(2) Å, respectively, which fall within the range of other complexes [46–48]. The N3 proton of coordinated isothioamide participates in a hydrogen bond (2.951(4) Å) and forms a dimer with $R_2^2(8)$ graph set (figure 5). Hydrogen bond distances and angles for all complexes are given in table 4.

4. Conclusion

We synthesized 5-bromo-2-hydroxybenzaldehyde *S*-allylisothiosemicarbazone hydrobromide (H_2L) as a tridentate NNO chelating agent. Neutral CuLIm, $CuLNH_3 \cdot 4H_2O$, and MoO_2L(1-MeIm) complexes were obtained by ligand reactions with an appropriate metal salt and imidazole (Im), NH_3 or 1-methylimidazole (1-MeIm). The compounds were fully characterized by elemental analyses, FT-IR, ^{1}H NMR, UV-Vis, TGA, and X-ray diffraction methods. The results show distorted square planar and octahedral geometry for copper and molybdenum complexes, respectively. H_2L is coordinated via phenolic hydroxyl, azomethine nitrogen, and nitrogen of isothioamide, forming six- and five-membered metallocycles. The thermogravimetric analyses showed that the complexes decompose *via* partial loss of the organic moiety, and finally the relevant metal oxides remained.

Supplementary material

Crystallographic data for the structures reported in this article have been deposited with the Cambridge Crystallographic Data Center as supplementary publication Nos. CCDC

871107-871109 for 1-3. TGA thermogram, FT-IR, ^{1}H NMR, and UV-Vis spectra of the compounds are presented in supplementary materials.

Acknowledgements

Reza Takjoo would like to thank the Ferdowsi University of Mashhad for supporting this work. We thank the Università di Messina (Italy) for the provision of a diffractometer.

References

[1] V.M. Leovac, V.I. Češljević. *Coordination Chemistry of Isothiosemicarbazides and their Derivatives*, Faculty of Sciences, University of Novi Sad, Novi Sad (2002).
[2] M. Freund, A. Schander. *Chem. Ber.,* **29**, 2500 (1896).
[3] Y.d. Kurt, B. Ülküseven, S. Tuna, M. Ergüven, S. Solakoğlu. *J. Coord. Chem.,* **62**, 2172 (2009).
[4] Y.D. Kurt, B. Ülküseven. *J. Coord. Chem.,* **63**, 828 (2010).
[5] M.S. Refat, I.M. El-Deen, Z.M. Anwer, S. El-Ghol. *J. Coord. Chem.,* **62**, 1709 (2009).
[6] N.V. Gerbeleu, V.B. Arion, J. Burgess. *Template Synthesis of Polyazamacrocyclic Compounds, in Template Synthesis of Macrocyclic Compounds*, Wiley-VCH Verlag GmbH, Weinheim (2007).
[7] M.T. Cocco, C. Congiu, V. Onnis, M.L. Pellerano, A. De Logu. *Bioorg. Med. Chem.,* **10**, 501 (2002).
[8] N. Amit, J. Rahul. *Curr. Med. Chem.,* **12**, 1873 (1886).
[9] B. Atasever, B. Ülküseven, T. Bal-Demirci, S. Erdem-Kuruca, Z. Solakoğlu. *Invest. New Drugs,* **28**, 421 (2010).
[10] M. Belicchi-Ferrari, F. Bisceglie, C. Casoli, S. Durot, I. Morgenstern-Badarau, G. Pelosi, E. Pilotti, P. Tarasconi. *J. Med. Chem.,* **48**, 1671 (2005).
[11] İ. Kizilcikli, Y.D. Kurt, B. Akkurt, A.Y. Genel, S. Birteksöz, B. Ülküseven. *Folia Microbiol.,* **52**, 15 (2007).
[12] H. Beraldo, D. Gambino. *Mini. Rev. Med. Chem.,* **4**, 31 (2004).
[13] D.K. Sau, R.J. Butcher, S. Chaudhuri, N. Saha. *Mol. Cell. Biochem.,* **253**, 21 (2003).
[14] A.P. Rebolledo, M. Vieites, D. Gambino, O.E. Piro, E.E. Castellano, C.L. Zani, E.M. Souza-Fagundes, L.R. Teixeira, H. Beraldo. *J. Inorg. Biochem.,* **99**, 698 (2005).
[15] C. Feng-Tai Chen, G.-R. Tang, G.-X. Jin. *J. Organomet. Chem.,* **692**, 3435 (2007).
[16] E.B. de Vargas, R.H. de Rossi. *Tetrahedron Lett.,* **23**, 4423 (1982).
[17] D.L. Pavia, G.M. Lampman, G.S. Kriz, J.A. Vyvyan. *Introduction to Spectroscopy*, 4th edn. Edn. Brooks/Cole, Minnesota (2008).
[18] Q. Wang, C.F. Bi, Y.H. Fan, X. Zhang, J. Zuo, S.B. Liu. *Russ. J. Coord. Chem.,* **37**, 228 (2011).
[19] M.L. Tong, L.J. Li, K. Mochizuki, H.C. Chang, X.M. Chen, S. Kitagawa. *Chem. Commun.,* **428**, (2003).
[20] P.B. King. *Encyclopedia of Inorganic Chemistry.* p. 829, John Wiley & Sons, New York, NY (1994).
[21] V.B. Arion, P. Rapta, J. Telser, S.S. Shova, M. Breza, J. Kožišek. *Inorg. Chem.,* **50**, 2918 (2011).
[22] N.R. Pramanik, S. Ghosh, T.K. Raychaudhuri, S. Ray, R.J. Butcher, S.S. Mandal. *Polyhedron,* **23**, 1595 (2004).
[23] B.E. Schultz, R. Hille, R.H. Holm. *J. Am. Chem. Soc.,* **117**, 827 (1995).
[24] D. Eierhoff, W.C. Tung, A. Hammerschmidt, B. Krebs. *Inorg. Chim. Acta,* **362**, 915 (2009).
[25] U. Sandbhor, S. Padhye, E. Sinn. *Transition Met. Chem.,* **27**, 681 (2002).
[26] (a) COSMO, version 1.60; Bruker AXS Inc.: Madison, Wisconsin (2005); (b) SAINT, version 7.06A; Bruker AXS Inc.: Madison, Wisconsin (2005); (c) SADABS, version 2.10; Bruker AXS Inc.: Madison, Wisconsin (2005).
[27] M.C. Burla, R. Caliandro, M. Camalli, B. Carrozzini, G.L. Cascarano, L. De Caro, C. Giacovazzo, R. Spagna. *SIR2004. J. Appl. Crystallogr.,* **38**, 381 (2005).
[28] G.M. Sheldrick. *SHELXL97*, University of Göttingen, Göttingen, Germany (1997).
[29] P. Larkin. *Infrared and Raman Spectroscopy; Principles and Spectral Interpretation*. p. 106, 1st edn Edn. Elsevier, Amsterdam (2011).
[30] R. Takjoo, M. Hakimi, M. Seyyedin, M. Abrishami. *J. Sulfur Chem.,* **31**, 41 (2010).
[31] V.M. Leovac, V.I. Češljević. *Polyhedron,* **7**, 2641 (1988).
[32] I. Yilmaz, A. Cukurovali. *Heterat. Chem.,* **14**, 617 (2003).
[33] D.-M. Xian, Z.-L. You, M. Zhang, P. Hou, X.-H. Li. *J. Coord. Chem.,* **64**, 3265 (2011).
[34] A.Y. Genel, B. Ülküseven, İ. Kızılcıklı. *Russ. J. Inorg. Chem.,* **53**, 1747 (2008).
[35] J.A. Dean. *Lange's Handbook of Chemistry*, 11th Edn. Edn, Wiley-VCH Verlag GmbH, Weinheim (2009)
[36] V.M. Leovac, V. Divjaković, M.D. Joksović, L.S. Jovanović, L.S. Vojinovic-jesiv, M. Mlinar. *J. Serb. Chem. Soc.,* **75**, 1063 (2010).

[37] M. Şahin, T. Bal-Demirci, G. Pozan-Soylu, B. Ülküseven. *Inorg. Chim. Acta,* **362**, 2407 (2009).
[38] D.X. West, Y. Yang, T.L. Klein, K.I. Goldberg, A.E. Liberta. *Polyhedron,* **14**, 3051 (1995).
[39] C. Yamazaki. *Can. J. Chem.,* **53**, 610 (1975).
[40] Z.D. Tomić, A. Kapor, A. Žmirić, V.M. Leovac, D. Zobel, S.D. Zarić. *Inorg. Chim. Acta,* **360**, 2197 (2007).
[41] S. Duman, I. Kızılcıklı, A. Koca, A.M. Akkurt, B. Ülküseven. *Polyhedron,* **29**, 2924 (2010).
[42] Ş. Güveli, B. Ülküseven. *Polyhedron,* **30**, 1385 (2011).
[43] R. Takjoo, R. Centore, M. Hakimi, S.A. Beyramabadi, A. Morsali. *Inorg. Chim. Acta,* **371**, 36 (2011).
[44] İ. Kızılcıklı, S. Eğlence, A. Gelir, B. Ülküseven. *Transition Met. Chem.,* **33**, 775 (2008).
[45] B.İ. Ceylan, Y.D. Kurt, B. Ülküseven. *J. Coord. Chem.,* **62**, 757 (2009).
[46] A.B. Ilyukhin, V.S. Sergienko, V.L. Zmiric, V.M. Abramenko. *Kristallografiya (Russ.), (Crystallogr. Rep.),* **39**, 843 (1994).
[47] A.B. Ilyukhin, V.S. Sergienko, V.L. Zmiric, V.M. Abramenko. *Kristallografiya (Russ.), (Crystallogr. Rep),* **41**, 678 (1996).
[48] Z.D. Tomic, A. Kapor, A. Zmiric, V.M. Leovac, D. Zobel, S.D. Zaric. *Inorg. Chim. Acta,* **360**, 2197 (2007).